Proceedings of the World Congress on Engineering 2014 Vol II,
WCE 2014, July 2 - 4, 2014, London, U.K.

A Study on the Distortion Correction Methodology of Vision Sensor

Younghoon Kho, Yongjin (James) Kwon

***Abstract*—This study investigates a simple and effective vision calibration method, which is suitable for use on the shop floor. Our method doesn't utilize expensive measuring equipment for complex alignment process between the robot and image planes. The vision calibration grid is designed with CAD software and printed on a piece of white paper, which can be easily duplicable on the shop floor. The proposed Jacobian method significantly improves the positioning accuracy of vision guided robotic operations, which appear to be far superior to the iVY calibration method provided by the robot manufacturer.**

***Index Terms*—Vision sensor, Yamaha iVY Robot Vision System, Jacobian matrix, Vision calibration**

I. Introduction

Many modern production processes are automated using vision sensors. Vision sensors make it possible to adapt to changes, and have wide applications by having integrated with robots. Because of the use of vision sensors, robotic assembly tasks can be conducted automatically with precision. However, one of the major problems of using vision sensors is that measured coordinates and real coordinates do not coincide due to lens distortion. Fig. 1 represents two types of lens distortion. One is a pincushion distortion and the other is a barrel distortion [1-3].

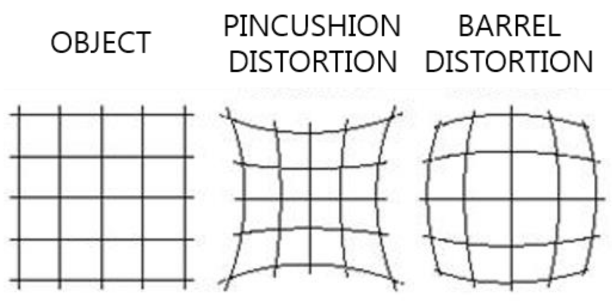

Fig 1. Two types of lens distortion

Many studies addressed the lens distortion problems, yet existing methods are not suitable enough in terms of simplicity and cost [4-7]. This study proposes a new methodology for the correction of lens distortion using the Yamaha iVY Robot Vision System.

Manuscript received March 14, 2014; revised March 31, 2014.

Younghoon Kho is with the Industrial Engineering of Ajou University, Suwon, Korea (corresponding author to provide phone: +82-10-9244-0677; e-mail: dotman87@ gmail.com).

Yongjin(James) Kwon is with the the Industrial Engineering of Ajou University, Suwon, Korea (corresponding author to provide phone: +82-31-219-2418; fax: +82-31-219-1610; e-mail: yk73@ajou.ac.kr).

II. Set-Up of The Study

A. *Yamaha iVY Robot Vision System*

Fig. 2 shows the Yamaha iVY Robot Vision System. The Channel 2 vision sensor is fixed on the ceiling, having a 8 mm TV lens with a magnification of 1.3. On the other hand, The Channel 1 vision sensor is attached on the robot arm, and moves with the robot arm motion. It has a 16 mm TV lens with a magnification of 1.4. Each vision sensor has a LED lighting control.

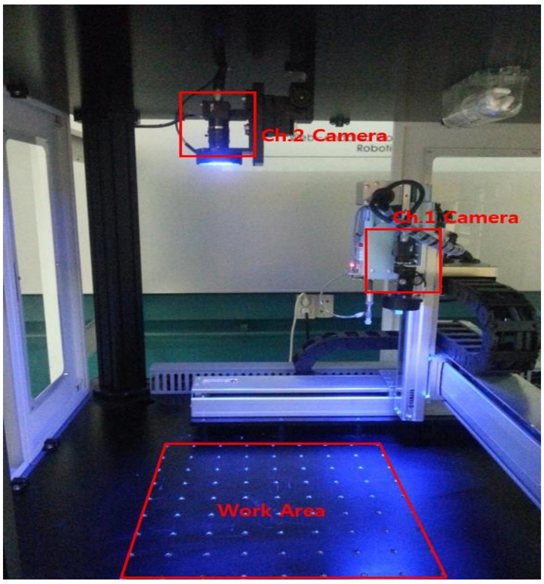

Fig 2. Yamaha iVY Robot Vision System

The iVY Studio is the operating software that manages the system via a personal computer. The iVY Studio has major functions as follows: registration of object to find; registration of fiducial mark for calibration; and setting the vision sensor's search area. Fig. 3 is an actual picture of the iVY Studio.

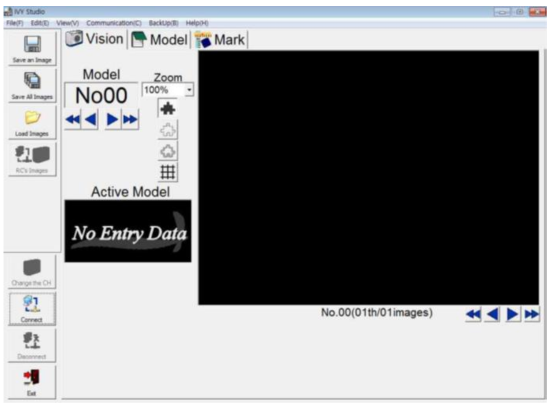

Fig 3. The iVY Studio

B. Register the Fiducial Mark on the iVY Studio

The iVY Studio provides its own calibration technique function. This is a set procedure within the system, to expedite the vision-robot calibration process on the shop floor. The iVY system is an integrated system, which connects both vision and robot platforms. Therefore, the end users don't have to go through a difficult task of making different platforms communicating with one another. The iVY Studio makes the calibration easy as well for the end users. It is required to register two fiducial marks first. Fig. 4 represents the fiducial marks. Fiducial marks have to locate on vision sensor's field of view, which should be reasonably set apart. Then, each fiducial mark's robot coordinate is measured and recorded through a teach pendent. Fig. 5 shows the process of the iVY calibration method.

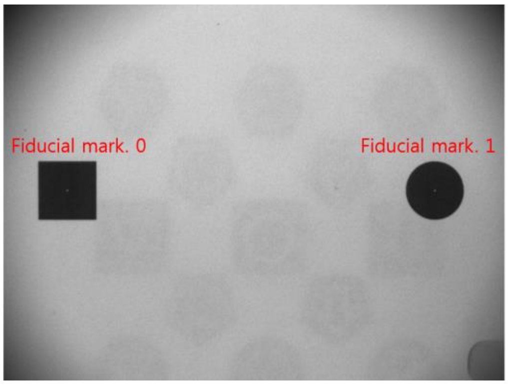

Fig 4. Fiducial marks for iVY calibration

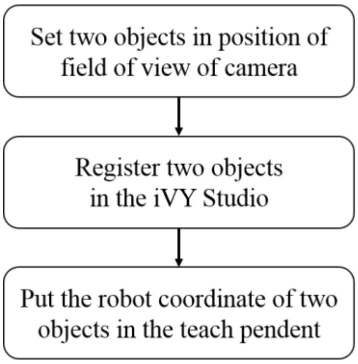

Fig 5. The process of the YAMAHA calibration method

III. Calibration with iVY System

A. Models used in the experiment

Before the experiment, one must register the model in the iVY Studio. Fig. 6 shows the models used in the experiment and each model has different shapes. Each model's width and height are 1.6 cm. There are 0.6 mm circles at the center of each model to make robot coordinate measurement simple.

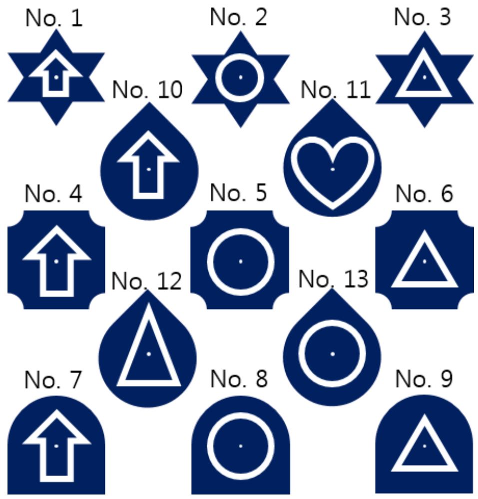

Fig 6. Models used in the experiment

B. Experiment with iVY calibration – CH.2 Camera

The iVY calibration is performed at three locations within the Channel 2 camera field of view (FOV): center, left and right areas of the FOV. Fig. 7 shows the images of the models positioned at three different locations within the CH.2 vision sensor's FOV.

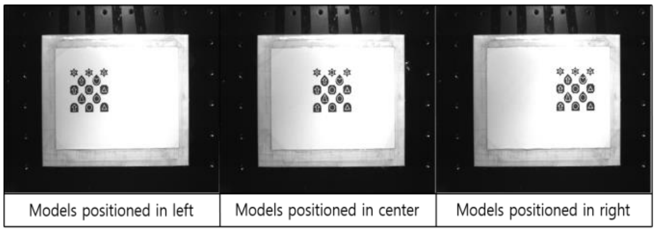

Fig 7. Models are measured at three positions in the CH. 2 FOV

Table. 1 represents the errors when model was positioned in the center of CH.2 FOV. The errors indicate the discrepancy between the iVY calibrated robot coordinates and the actual robot coordinates. The robot was manually adjusted, after the robot was vision guided to each model, in order to find out the discrepancy. Table. 2 represents the error that occurred when model was positioned in the left area of CH.2 FOV. Table. 3 represents the error of models positioned in right area of CH.2 vision sensor.

Table I
Errors (mm) in the center area - CH.2 Vision Sensor

Model Number	Measured Coordinate		Actual Coordinate		Error	
	X	Y	X	Y	X	Y
No. 1	221.75	145.90	221.37	146.07	0.38	0.17
No. 2	221.76	171.66	221.40	171.51	0.36	0.15
No. 3	222.20	197.41	221.45	197.09	0.75	0.32
No. 4	247.50	146.24	246.83	146.03	0.67	0.21
No. 5	247.16	171.43	246.92	171.52	0.24	0.09
No. 6	247.38	197.17	247.02	196.99	0.36	0.18
No. 7	273.25	146.03	272.43	145.84	0.82	0.19
No. 8	272.91	171.78	272.51	171.43	0.40	0.35
No. 9	273.70	197.53	272.61	196.95	1.09	0.58
No. 10	234.45	158.94	234.09	158.79	0.36	0.15
No. 11	233.53	184.14	234.17	184.24	0.64	0.10
No. 12	259.64	158.73	259.67	158.75	0.03	0.02
No. 13	259.29	184.49	259.68	184.21	0.39	0.28
				Average	**0.50**	**0.21**

ISBN: 978-988-19253-5-0
ISSN: 2078-0958 (Print); ISSN: 2078-0966 (Online)

Table II
Errors (mm) in the left area - CH.2 Vision Sensor

Model Number	Measured Coordinate		Actual Coordinate		Error	
	X	Y	X	Y	X	Y
No. 1	220.84	101.31	220.72	101.24	0.12	0.07
No. 2	220.86	126.61	220.97	126.77	0.11	0.16
No. 3	221.69	152.39	221.29	152.38	0.40	0.01
No. 4	247.08	100.88	246.65	101.13	0.43	0.25
No. 5	246.70	126.26	246.85	126.67	0.15	0.41
No. 6	247.35	152.01	247.01	152.18	0.34	0.17
No. 7	272.96	101.09	272.31	100.87	0.65	0.22
No. 8	273.06	127.12	272.40	126.48	0.66	0.64
No. 9	273.28	152.27	272.58	152.05	0.70	0.22
No. 10	233.27	113.55	233.94	113.93	0.67	0.38
No. 11	233.82	139.25	234.03	139.52	0.21	0.27
No. 12	259.11	113.56	259.56	113.78	0.45	0.22
No. 13	258.84	139.29	259.71	139.40	0.87	0.11
				Average	**0.44**	**0.24**

Table III
Errors (mm) in the right area - CH.2 Vision Sensor

Model Number	Measured Coordinate		Actual Coordinate		Error	
	X	Y	X	Y	X	Y
No. 1	220.94	193.72	221.74	193.78	0.80	0.06
No. 2	220.83	218.92	221.82	219.36	0.99	0.44
No. 3	221.37	244.83	221.91	244.99	0.54	0.16
No. 4	246.77	193.49	247.49	193.82	0.72	0.33
No. 5	246.49	219.07	247.52	219.38	1.03	0.31
No. 6	247.02	244.76	247.58	244.99	0.56	0.23
No. 7	272.36	193.32	272.95	193.82	0.59	0.50
No. 8	272.05	218.88	273.04	219.34	0.99	0.46
No. 9	272.64	244.74	273.10	244.92	0.46	0.18
No. 10	234.01	206.14	234.62	206.59	0.61	0.45
No. 11	233.71	231.97	234.71	232.05	1.00	0.08
No. 12	259.33	206.26	260.23	206.6	0.90	0.34
No. 13	259.04	231.92	260.24	232.19	1.20	0.27
				Average	**0.80**	**0.29**

Fig. 8 and Fig. 9 show the errors along the robot X and Y directions for Channel 2.

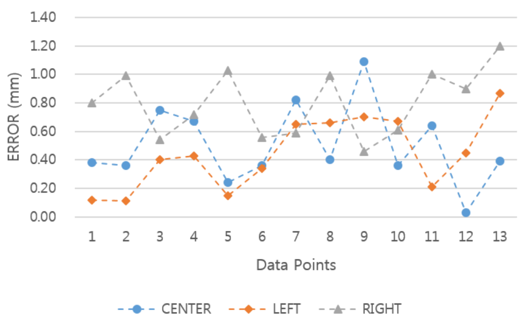

Fig 8. X-axis errors of the CH.2 vision sensor

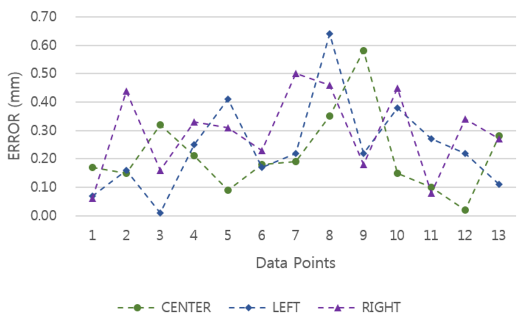

Fig 9. Y-axis error of the CH.2 vision sensor

C. Experiment with iVY calibration – CH.1 Camera

For the second experiment, the iVY calibration is performed at three locations for the Channel 1 camera. Fig. 10 shows the CH.1 vision sensor's FOV for each location.

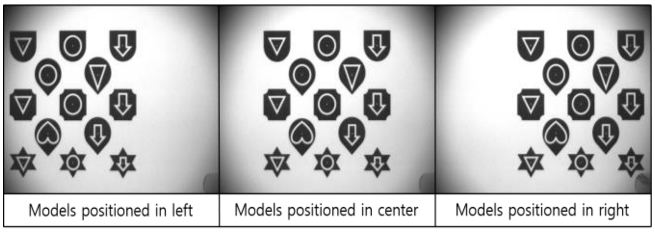

Fig 10. Models are measured at three positions in the CH. 1 FOV

Table. 4 represents the errors that occurred when model was positioned in the center area of CH.1 FOV. Table. 5 represents the errors for the left area. Table. 6 represents the errors for the right area of CH.1 FOV.

Table IV
Errors (mm) in the center area - CH.1 Vision Sensor

Model Number	Measured Coordinate		Actual Coordinate		Error	
	X	Y	X	Y	X	Y
No. 1	220.97	145.85	221.37	146.07	0.40	0.22
No. 2	221.07	171.39	221.40	171.51	0.33	0.12
No. 3	221.69	197.07	221.45	197.09	0.24	0.02
No. 4	246.84	145.97	246.83	146.03	0.01	0.06
No. 5	246.58	171.48	246.92	171.52	0.34	0.04
No. 6	247.20	197.12	247.02	196.99	0.18	0.13
No. 7	272.52	145.70	272.43	145.84	0.09	0.14
No. 8	272.44	171.24	272.51	171.43	0.07	0.19
No. 9	272.88	196.82	272.61	196.95	0.27	0.13
No. 10	234.13	158.61	234.09	158.79	0.04	0.18
No. 11	233.88	184.29	234.17	184.24	0.29	0.05
No. 12	259.47	158.69	259.67	158.75	0.20	0.06
No. 13	259.22	184.20	259.68	184.21	0.46	0.01
				Average	**0.22**	**0.10**

Table V
Errors (mm) in the left area - CH.1 Vision Sensor

Model Number	Measured Coordinate		Actual Coordinate		Error	
	X	Y	X	Y	X	Y
No. 1	220.44	101.38	220.72	101.24	0.28	0.14
No. 2	220.50	126.58	220.97	126.77	0.47	0.19
No. 3	221.25	152.25	221.29	152.38	0.04	0.13
No. 4	246.26	100.99	246.65	101.13	0.39	0.14
No. 5	246.34	126.52	246.85	126.67	0.51	0.15
No. 6	246.86	151.98	247.01	152.18	0.15	0.20
No. 7	271.87	100.61	272.31	100.87	0.44	0.26
No. 8	271.92	126.31	272.40	126.48	0.48	0.17
No. 9	272.43	151.79	272.58	152.05	0.15	0.26
No. 10	233.59	113.70	233.94	113.93	0.35	0.23
No. 11	233.44	139.41	234.03	139.52	0.59	0.11
No. 12	259.16	113.65	259.56	113.78	0.40	0.13
No. 13	259.24	139.19	259.71	139.40	0.47	0.21
				Average	**0.36**	**0.18**

Table VI
Errors (mm) in the right area - CH.1 Vision Sensor

Model Number	Measured Coordinate		Actual Coordinate		Error	
	X	Y	X	Y	X	Y
No. 1	221.03	193.97	221.74	193.78	0.71	0.19
No. 2	221.01	219.51	221.82	219.36	0.81	0.15
No. 3	221.83	245.26	221.91	244.99	0.08	0.27
No. 4	247.35	193.75	247.49	193.82	0.14	0.07
No. 5	246.87	219.26	247.52	219.38	0.65	0.12

ISBN: 978-988-19253-5-0
ISSN: 2078-0958 (Print); ISSN: 2078-0966 (Online)

No. 6	247.07	245.05	247.58	244.99	0.51	0.06
No. 7	273.10	194.10	272.95	193.82	0.15	0.28
No. 8	273.21	220.26	273.04	219.34	0.17	0.92
No. 9	273.24	245.45	273.10	244.92	0.14	0.53
No. 10	234.29	206.46	234.62	206.59	0.33	0.13
No. 11	233.96	232.20	234.71	232.05	0.75	0.15
No. 12	259.29	206.61	260.23	206.60	0.94	0.01
No. 13	258.91	232.40	260.24	232.19	1.33	0.21
				Average	**0.52**	**0.24**

Fig. 11 and Fig. 12 show the errors along the robot X and Y directions for Channel 1.

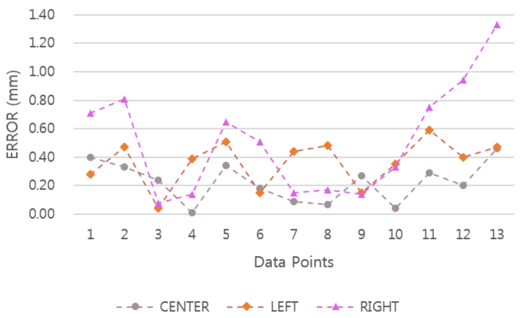

Fig 11. X-axis errors of the CH.1 vision sensor at each position

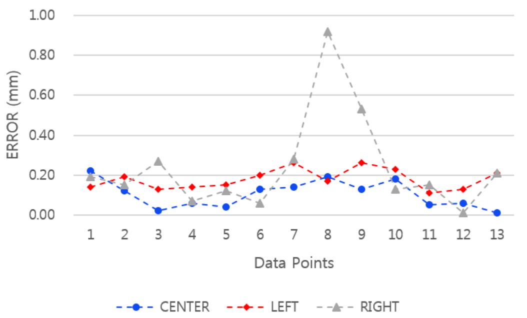

Fig 12. Y-axis errors of the CH.1 vision sensor at each position

IV. Calibration Using Jacobian Matrix

A. *Jacobian Matrix*

Robot control using an image can be viewed as a conversion between the robot coordinate system and pixel coordinate system [1-4]. To describe mathematically, $T = \mathbb{R}^2 \rightarrow \mathbb{R}^2$ represents the coordinate transformation that is based on the Euclidian [5-8]. It can be expressed as $T_{(u,v)} = (x_{(u,v)}, y_{(u,v)})$. At this time, $\frac{\partial(x,y)}{\partial(u,v)} = \det DT_{(u,v)}$.

In robot control using a vision, variable x and y turn out to be u and v, since it is a conversion of pixel coordinate into robot coordinate. In the center of the image, lens distortion tends to be minimal, while the distortion increases towards the corner areas of the image. This phenomenon can be clearly observed, based on the experiment data. The Jacobian calibration method is described in Fig. 13.

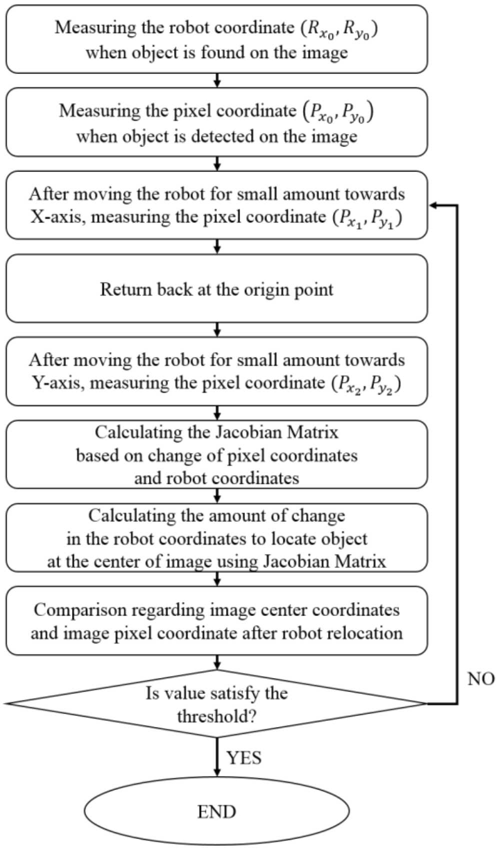

Fig 13. Calibration process using Jacobian Matrix

B. *Experimental result*

Table. 7 ~ Table. 8 represent the result of experiment using Jacobian Matrix.

Table VII
Errors (mm) in the center area - Using Jacobian Matrix

Model Number	Measured Coordinate		Actual Coordinate		Error	
	X	Y	X	Y	X	Y
No. 1	221.34	146.04	221.37	146.07	0.03	0.03
No. 2	221.38	171.48	221.40	171.51	0.02	0.03
No. 3	221.44	197.13	221.45	197.09	0.01	0.04
No. 4	246.80	145.97	246.83	146.03	0.03	0.06
No. 5	246.98	171.54	246.92	171.52	0.06	0.02
No. 6	247.07	196.89	247.02	196.99	0.05	0.1
No. 7	272.42	145.75	272.43	145.84	0.01	0.09
No. 8	272.48	171.40	272.51	171.43	0.03	0.03
No. 9	272.59	196.89	272.61	196.95	0.02	0.06
No. 10	234.03	158.85	234.09	158.79	0.06	0.06
No. 11	234.19	184.21	234.17	184.24	0.02	0.03
No. 12	259.70	158.68	259.67	158.75	0.03	0.07
No. 13	259.71	184.25	259.68	184.21	0.03	0.04
				Average	**0.03**	**0.05**

Table VIII
Errors (mm) in the left area - Using Jacobian Matrix

Model Number	Measured Coordinate		Actual Coordinate		Error	
	X	Y	X	Y	X	Y
No. 1	220.69	101.19	220.72	101.24	0.03	0.05
No. 2	220.96	126.83	220.97	126.77	0.01	0.06
No. 3	221.27	152.30	221.29	152.38	0.02	0.08
No. 4	246.58	101.14	246.65	101.13	0.07	0.01
No. 5	246.89	126.58	246.85	126.67	0.04	0.09
No. 6	246.92	152.11	247.01	152.18	0.09	0.07
No. 7	272.30	100.84	272.31	100.87	0.01	0.03
No. 8	272.35	126.50	272.40	126.48	0.05	0.02
No. 9	272.52	152.03	272.58	152.05	0.06	0.02
No. 10	233.91	113.94	233.94	113.93	0.03	0.01

ISBN: 978-988-19253-5-0
ISSN: 2078-0958 (Print); ISSN: 2078-0966 (Online)

No. 11	234.04	139.48	234.03	139.52	0.01	0.04
No. 12	259.58	113.73	259.56	113.78	0.02	0.05
No. 13	259.78	139.37	259.71	139.40	0.07	0.03
				Average	**0.04**	**0.04**

Table IX
Errors (mm) in the right area - Using Jacobian Matrix

Model Number	Measured Coordinate		Actual Coordinate		Error	
	X	Y	X	Y	X	Y
No. 1	221.68	193.77	221.74	193.78	0.06	0.01
No. 2	221.80	219.31	221.82	219.36	0.02	0.05
No. 3	221.88	244.96	221.91	244.99	0.03	0.03
No. 4	247.43	193.78	247.49	193.82	0.06	0.04
No. 5	247.48	219.37	247.52	219.38	0.04	0.01
No. 6	247.54	244.98	247.58	244.99	0.04	0.01
No. 7	272.94	193.80	272.95	193.82	0.01	0.02
No. 8	273.03	219.28	273.04	219.34	0.01	0.06
No. 9	273.01	244.90	273.10	244.92	0.09	0.02
No. 10	234.58	206.55	234.62	206.59	0.04	0.04
No. 11	234.70	232.01	234.71	232.05	0.01	0.04
No. 12	260.18	206.55	260.23	206.60	0.05	0.05
No. 13	260.22	232.16	260.24	232.19	0.02	0.03
				Average	**0.04**	**0.03**

Fig. 14 and Fig. 15 show the X and Y errors of vision calibration using the Jacobian calibration method.

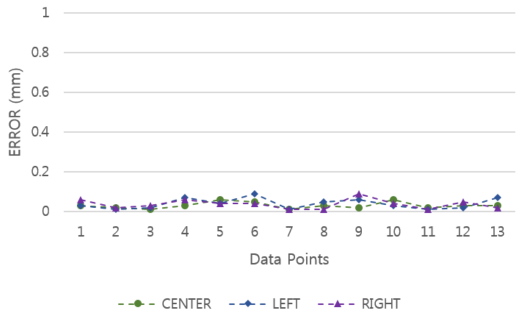

Fig 14. X-coordinate errors of CH.1 vision sensor at each position

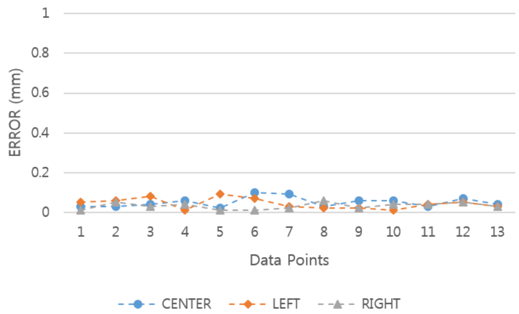

Fig 15. Y-coordinate errors of CH.1 vision sensor at each position

V. Result

Based on the experimental result, a capability analysis is performed for the robot X-axis and Y-axis. Table. 10 shows the capability analysis for the X and Table. 11 represents the Y-axis. Fig. 16 and Fig. 17 show the graphical representation, which clearly manifest the significant reduction of the calibration errors using the Jacobian method. The substantial improvement of positioning accuracy is evident, and the spread between the data points has been greatly reduced, which shows a very stable and consistent pattern. Even using a calibration models printed on a piece of white paper, the proposed method performs far better than the iVY method. The proposed method can be better suited for industrial applications due to simplicity and ease of adaptation on the shop floor.

Table X
Capability Analysis for X-axis

CH.2 Vision Sensor		CH.1 Vision Sensor		Jacobian Matrix	
USL	2	USL	2	USL	2
LSL	0	LSL	0	LSL	0
Average	0.581	Average	0.368	Average	0.036
Stdev	0.292	Stdev	0.273	Stdev	0.022
3σ	0.875	3σ	0.820	3σ	0.066
Cp	1.143	Cp	1.219	Cp	15.039

Table XI
Capability Analysis for Y-axis

CH.2 Vision Sensor		CH.1 Vision Sensor		Jacobian Matrix	
USL	2	USL	2	USL	2
LSL	0	LSL	0	LSL	0
Average	0.249	Average	0.173	Average	0.042
Stdev	0.149	Stdev	0.153	Stdev	0.024
3σ	0.446	3σ	0.459	3σ	0.071
Cp	2.240	Cp	2.178	Cp	14.172

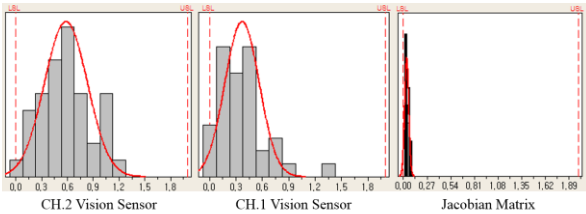

Fig 16. Process Capability of X-axis

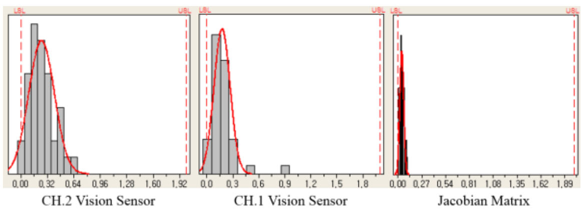

Fig 17. Process Capability of Y-axis

References

[1] Tasi, R. Y., "A versatile camera calibration technique for high-accuracy 3D machine vision metrology using off-the-shelf TV cameras and lenses," *IEEE Trans. Robot. Automat.*, vol. 3, no. 4, pp. 323-344, Aug. 1987.

[2] Lyndon N. Smith, Melvyn L. Smith, "Automatic Machine vision calibration using statistical and neural network methods," *Image and vision Computing*, vol. 23, issue 10, Sep. 2005.

[3] Zhengyou Zhang, "A flexible new technique for camera calibration," *IEEE Trans. Pattern Anal. Machine Intell.*, vol. 22, no. 11, pp. 1330-1334, Nov. 2000.

[4] David Liebowitz and Andrew Zisserman, "Combining scene and auto-calibration constraints," in *Proc. IEEE International Conference on Computer Vision*, Kerkyra, Greece, Sept. 1999, pp. 293-300.

[5] Jun-Sik Kim and In So Kwon, "Estimating intrinsic parameters of cameras using two arbitrary rectangles," in *Proc. International Conference on Pattern Recognition*, Hong Kong, Aug. 2006.

[6] Marc Pollefeys, "Visual modeling with a handheld camera," *International Journal of Computer Vision*, vol. 59, no. 3, pp. 207-232, Oct. 2004.

[7] Xianghua Ying and Hongbin Zha, "Geometric interpretations of the relation between the image of the absolute conic and sphere images," *IEEE Trans. Pattern Anal. Machine Intell*., vol. 28, no. 12, pp. 2031-2036, Dec. 2006.

[8] Marta Wilczkowiak, Peter Sturm, and Edmond Boyer, "Using geometric constraints through parallelepipeds for calibration and 3D modelling," *IEEE Trans. Pattern Anal. Machine Intell*., vol. 27, no. 2, pp. 194-207, Feb. 2005.

ISBN: 978-988-19253-5-0
ISSN: 2078-0958 (Print); ISSN: 2078-0966 (Online)